

Research on Bending Behavior of Transmission Tower's X-type Multiple Ring Plate Joints with Annular Plane

Xiang Li¹, Xiaolu Li², Xinwu Wang^{2*}, Yongqiang Yu¹, Yan Zhao² and Jingkang Cheng³

¹College of Civil Engineering, Henan Polytechnic University, Henan Jiaozuo, China

²College of Civil Engineering, Luoyang Institute of Science and Technology, Henan Luoyang, China

³College of Civil Engineering, Henan University of Science and Technology, Henan Luoyang, China

Abstract: Tube-plate joints have been increasingly used in steel tubular tower structures. Addition of two or more ring-shaped reinforcing plates could not only decrease stress concentration, but also improve the load-bearing performance of tube-plate joints. In this research, we investigated the damage mode and bending resistance of steel pipe multi-ring plate nodes through simulating and analyzing three-ring, four-ring, and five-ring planar X-nodes. Simulation results proved that for the bending condition of X-type node, setting four ring plates was the best method for improving load capacity; and it was not recommended to set ring plates at the symmetry axis position of the node plate. Plasticity theory and regression analysis method were applied to derive equations for the flexural load capacity of multi-ring plate nodes.

Keywords: Steel pipe tower; Multi-ring plate node; Bending property; Bearing capacity

1. Introduction

The steel tube tower has the advantages of small size factor, simple structure, and clear sight of force transmission, so it is more used in the extra-high voltage transmission line. The connection structure and bearing capacity of the nodes are related to the safety of the whole tower and even the entire line project. The node structure of the transmission tower is a crucial step in tower design.

Liu et al.[1,2] performed an experimental research on annular plate stiffened rib transmission tower nodes, proposed an analytical model to estimate the ultimate bearing capacity of steel tube annular rib nodes, and derived the bending ultimate bearing capacity equation for inserted plate nodes on the basis of energy theory and the principle of virtual work. Bai et al.[3] performed an experimental research on the ultimate bearing capacity of 1/4 and 1/2 ring type plus rib steel pipe insert nodes ; and determined node ultimate bearing capacity through numerical analysis. Lv et al.[4] conducted experimental and finite element analyses on the ultimate bearing capacity of 1/4 ring plates and no ring plate steel pipe tower nodes and explored the effects of different ring plate parameters on the ultimate bearing capacity of nodes. Li et al.[5,6] performed foot-rule tests on 1/4 ring ribbed KT-type and full ring plate X-type nodes to determine the ultimate strength of KT-type and X-type nodes and derived design fitting equation and modified design equation for KT-type nodes. Li et al.[7,8] performed experimental and numerical calculations on 1/4 ring plus rib K-type nodes and 1/2 ring ribbed DK-type space. Damage form and bearing capacity of DK space nodes were studied and an empirical equation was derived for the design bearing capacity of DK space nodes. The obtained results showed that annular plates could improve the moment-bearing capacity and deformation capacity of K-type and DK-type nodes. Ju et al. [9] undertook static tests on nodes connected with ribbed K-type nodal plates to investigate their ultimate bearing capacity and derived an equation for the bearing capacity of K-type nodes. Qu et al.[10] studied the ultimate performance of high-strength steel tube-nodal plates connected with annular ribbed plates. Ultimate node performance was experimentally and numerically investigated, the force performance and damage mode of K-type nodes were studied, and prediction equation for ultimate flexural load capacity of K-type nodes with ring-type rib plate was derived based on energy theory. Yang et al.[11,12] performed foot tests on the bending performance of 90° and 180° nodes of steel pipe tower ring-type plus ribs, derived an equation for the calculation of flexural bearing capacity according to plasticity theory and regression analysis and determined the interactions of ultimate strength and normal stress of main material. Yang took the node at the main material of steel tube tower cross-stretcher as research object, performed force and buckling analyses of various size models, and investigated the influences of different geometric parameters on the ultimate bearing capacity and damage mode of the structure [13]. Zhang et al.[14] performed an experimental research and finite element analysis on the node connecting Ultra High Vacuum cross-beam to the large diameter coherent steel pipe of the tower and investigated the influence of ring-type stiffening ribs on node bearing capacity, stiffness, nodal plate, and nodal failure mode characteristics. Kim et al.[15] performed a parametric analysis on the plate - circular longitudinal hollow section X-type nodes exposed to in-plane bending-load; and derived the modified strength equation. Wang[16] studied the bending performance of K-type nodes through a combination of static tests and

finite element analyses and derived a calculation equation for the bending load capacity of K-type nodes based on the findings of experimental tests and theoretical analysis.

As illustrated in Fig. 1, multi-ring plate reinforced tube plate node is one of the most commonly used node forms in transmission tower structures. In summary, few studies have been conducted on the bending performance of multi-ring plate nodes, and the related design codes are not perfect. In this research, the bending performance of multi-ring plate nodes (two-ring, three-ring, four-ring, and five-ring plates) has been investigated by finite element analysis to obtain the damage mode and bending bearing capacity of the nodes. The proposed equation for flexural bearing capacity of multi-ring plate nodes was derived using theoretical analysis and regression analysis methods.

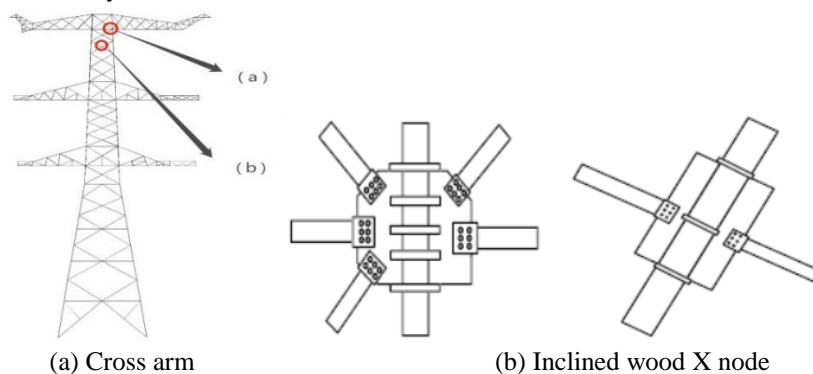


Fig.1 Connecting nodes of transmission towers

2. Establishment of finite element model

2.1. Finite element model

Refinement of finite element model and the underlying assumptions directly affected calculation results. As shown in Fig. 2, the finite element model of the node was developed to explore the static performance of the node. In this work, the finite element analysis software ABAQUS was applied and the unit used for finite element model of X-type node was C3D8R. The constraints, loading form, and mesh division; are illustrated in Fig. 2.

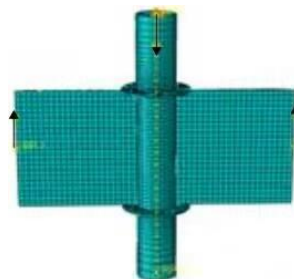


Fig.2 Finite element analysis model of X-type node1

2.2. Analysis Parameters

Fig. 3 illustrates the main parameters influencing the bearing capacity of X-node model. The main parameters included main tube diameter D , main tube wall thickness t_0 , ring plate height R , ring plate thickness t_r , node plate height B , node plate thickness t , and node plate angle β . The influences of the above parameters on the flexural performance of the node were evaluated separately.

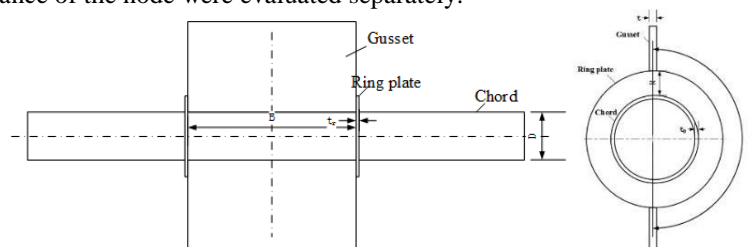


Fig.3 Parameters of X-type node model

2.3. Verification of finite element model

A total of four groups of 12 ring-type plus-ribbed nodes were adopted for experimental, tests according to reference [1], considering two nodal plate connection types, three steel pipe sizes, and two steel pipe materials. To verify the accuracy of finite element analysis method, the specimen of which ring-type double-sided ribbed was considered as verification target for comparative analysis in this, research and the dimensions of the selected nodes were as follows: main tube size $\phi 219 \times 6 \text{mm}$, length 1500mm; ring-type ribbed node size $\phi 80.5 \times 12 \text{mm}$; and node plate thickness 16mm, width 657mm. In this research, a finite element model with the same dimensions, materials, boundary conditions, and loading methods was developed based on the test results of member 1Qd in reference [1]. The yield strength of the main tube, ring plate, and node plate was 418 MPa, ultimate tensile strength was 520 MPa, Poisson's ratio was 0.3, elasticity modulus was 198 kN/mm², and elongation was 18%.

Fig.4 compares the simulation results of this research and experimental findings reported in reference [1]. From Fig. 4a, it was seen that the two load curves were in good agreement. Based on Figs. 4b and 4c, local buckling of steel tube at junction with nodal plate was observed in both simulation and test results, with a slight inversion of steel tube at upper end, a severe deformation of ring plate, and a slight bulging of steel tube at the lower end of the junction. In summary, the failure modes of node in experimental tests and simulations were consistent, indicating that establishing method of stiffened node model and the analysis results obtained from this research were reasonable.

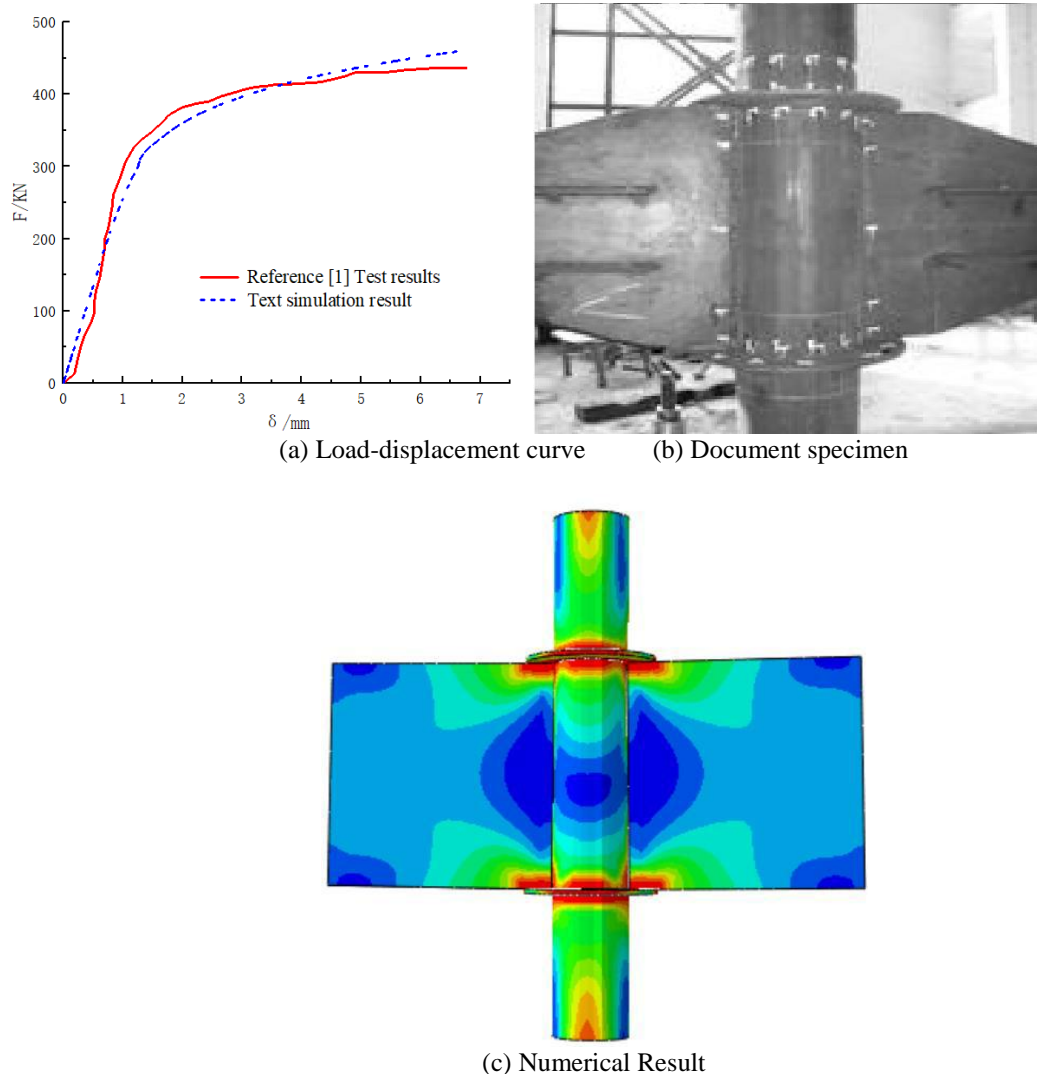


Fig.4 Comparative analysis of the results of numerical simulations of this work and experimental findings of reference [1]

3. Failure mode of X-type multiple ring plate nodes

Typical size nodes were adopted with $D=219\text{mm}$, $t_0=6\text{mm}$, $R=80.5\text{mm}$, $t_r=12\text{mm}$, $t=16\text{mm}$, $\beta=180^\circ$ constant, different nodal plate widths B , and different numbers of high ring plates n to investigate the flexural performance of each node. Fig. 7 illustrates the results of load bearing capacity of nodes with different nodal plate widths and ring plate numbers. Figs. 5 and 6 illustrate the deformation and stress distribution of nodes when X-node reached flexural bearing capacity with different node plate widths and ring plate numbers, respectively.

From Figs. 5 and 6, it was seen that: (1) When only ring plates were set on both sides of the node plate, the load of the node was mainly borne by ring plate; and the main material near the ring plate, and stress near the ring plate and ring plate basically reached 400 MPa when the node was damaged, and the material basically reached the yield-state. (2) When three or more ring plates were set, stress values near ring plates on both sides were higher and basically reached the yield strength of material when the node was damaged; however, the middle ring plate basically presented no deformation. This indicated that, for the case where the node was subjected to in-plane bending moment, setting the ring plate in the middle of the node plate could not share the load on the node. Furthermore, combined with the bearing capacity results illustrated in Fig. 7, it was found that the three-rings did not significantly improve bearing capacity compared with the two rings, but the four-rings improved bearing capacity by 22 % compared with three link points. This meant that the middle ring plate basically did not share the moment load on the node and had slight influence on the ultimate bearing capacity of the node. In summary, for the working condition of X-type node under bending moment, it was recommended to set four-ring plates.

In conclusion, it was suggested to set four-ring plates when X-type node was under bending moment.

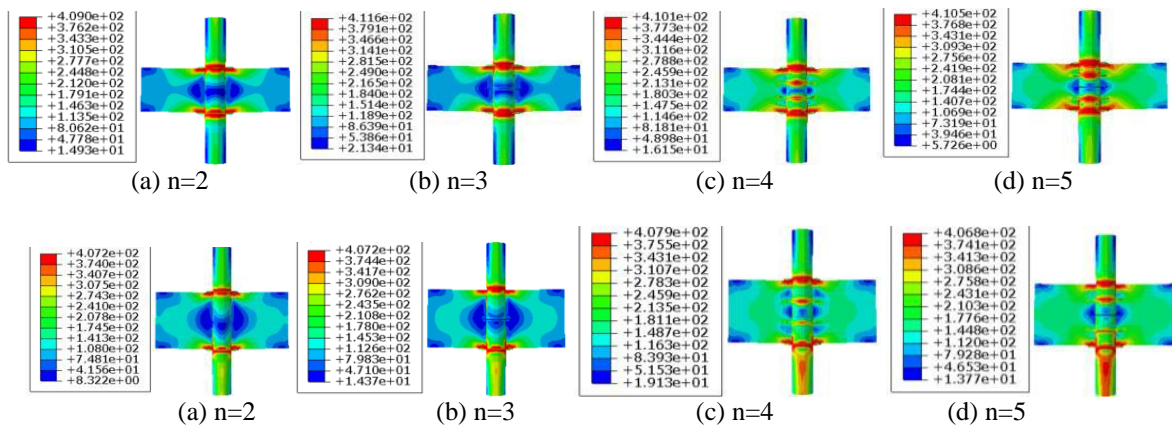


Fig.6 B=657mm failure modes of X nodes in different n scenarios

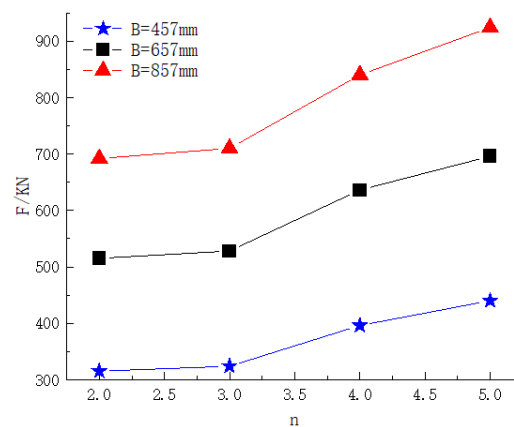


Fig.7 Bearing capacity of different ring plate numbers with different widths of node plates

4. Calculation of bearing capacity of X-type multiple ring plate joints

Based on simulation results, when X-shaped node was subjected to a bending moment, the applied load was mainly borne by each ring plate and the nearby main material. As shown in Fig. 8, first, the applied load F was equated to bending moment M and shear force Q acting on node plate: the bending moment applied to the node was equated to each ring plate:

$$M = F \cdot h \tag{1}$$

$$Q = F \tag{2}$$

Second, bending moment M was equated to the force acting on ring plate:

$$2P_1x_1 + 2P_2x_2 = M \tag{3}$$

Where x_i is the distance from ring plate to the centerline of node plate.

Ring plate was considered as the main resistance mechanism of the node, and the forces on the node plate could be simplified as shown in Fig 9. Since each ring plate had the same size, four-ring plates could be simplified to four springs with stiffness k. Therefore,

$$P_i = ky_i \tag{4}$$

$$\frac{P_2}{P_1} = \frac{y_2}{y_1} \tag{5}$$

As illustrated in Fig. 9, under the action of bending moment M, node plate was deformed to a certain extent, and the straight line below it became a deflection line. According to simulation results, the deflection y_i of the lower edge of node plate at each ring plate was obtained. This place makes

$$\eta = \frac{x_2}{B/2} \quad \frac{P_2}{P_1} = f(\eta) \tag{6}$$

Simulation results are presented in Fig. 10. Regression analysis yielded:

$$f(\eta) = 0.0214 + 1.2316\eta + 0.2281\eta^2 - 0.4711\eta^3 \quad R^2 = 0.995 \tag{7}$$

Eqs. (3) and (6) were combined to determine the nodal plate bending conditions. The bearing capacity of each ring plate was calculated as follows:

$$\begin{cases} 2P_1x_1 + 2P_2x_2 = M \\ \frac{P_1}{P_2} = \frac{y_1}{y_2} \end{cases} \tag{8}$$

According to the above equation, the load carried by each ring plate was calculated when the nodal plate was subjected to bending. Furthermore, the derived equation for the bearing capacity of a single ring plate was obtained from reference [6] for the design of the dimensions of each ring plate.

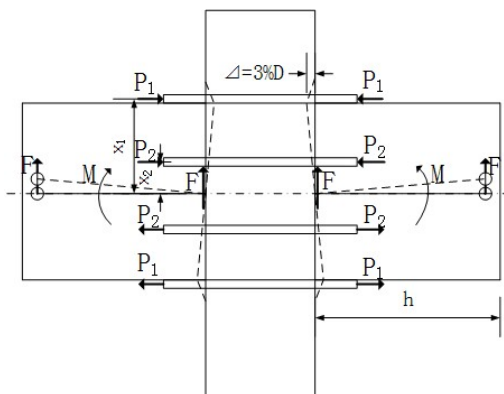


Fig.8 Node load decomposition

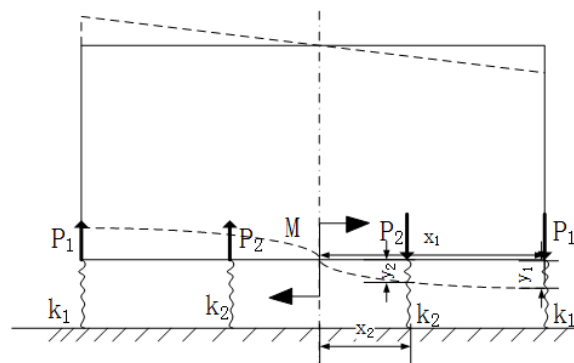


Fig.9 Joint equivalent load

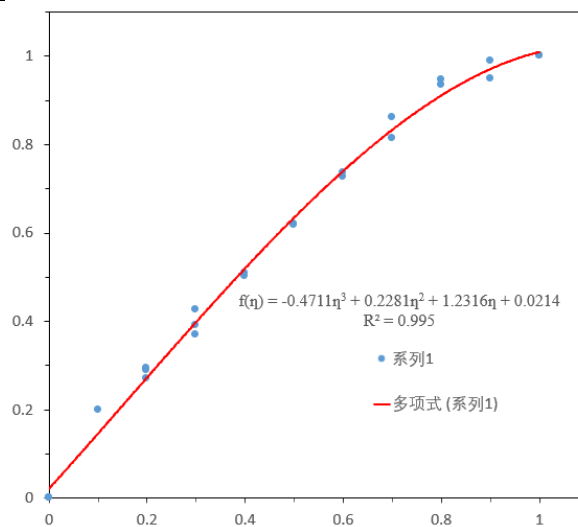


Fig.10 Regression analysis of load on ring plate

5. Conclusion

In this research, based on the review of the existing literature (two-ring plate), transmission steel pipe tower multi-ring plate nodes (three-ring, four-ring, and five-ring versions), and bending performance of finite element parametric analysis, the following conclusions were drawn:

- (1) The analysis results of the finite element model were compared with available test results; in literature and their overlap between was high, indicating that the developed finite element model was reasonable.
- (2) Setting multiple-ring plates improved the bending bearing capacity of X-shaped nodes of steel pipe transmission towers. When the node was subjected to bending moment load, setting four-ring plates significantly improved node bearing capacity, while it was not recommended to set ring plates on the symmetry axis of node plates.
- (3) We combined the results of simulation analyses, plasticity theory, and regression analyses to propose develop a method for calculating the load capacity distribution of each ring plate at multi-ring plate nodes, which could be applied to guide the design of multiple-ring plate sizes.

References

- [1]. Liu HJ, Li ZL, Li MH. (2010) Study on the ultimate load carrying capacity of steel tube transmission tower ring type plus rib node [J]. *Engineering Mechanics*, 27(10):65-73.
- [2]. Liu HJ, Li ZL. (2011) Study on the bending performance of inserted plate connection nodes based on steel tube control [J]. *Journal of Civil Engineering*, 44(02):21-27.
- [3]. Bai Q, Zeng DS, Shu AQ, Li ZL. (2012) Bearing analysis of annular ribbed nodes of steel tube transmission towers [J]. *Building Structure*, 42(02):103-106.
- [4]. Lv BH, Chen ZQ, Li H, Guan SQ, Li XL, Zhang L. (2012) Research on the Ultimate Bearing Capacity for Steel Tubular Transmission Tower's Joints with Annular Plate [J]. *Applied Mechanics and Materials*, 1799(166-169).
- [5]. Li XL, Zhang L, Xue XM, Wang XM, Wang HC. (2018) Prediction on ultimate strength of tube-gusset KT-joints stiffened by 1/4 ring plates through experimental and numerical study [J]. *Thin-Walled Structures*, 123.
- [6]. Li XL, Xue XM, Wang XM, Zhang L. (2021) Effect of chord compression on the ultimate strength of ring stiffened tube-gusset KT-type and X-type joints [P]. Luoyang Institute of Science and Technology (China); Xi'an Jiaotong Univ. (China); Northwest Electric Power Design Institute Co., Ltd. (China).
- [7]. Li F, Deng HZ, Hu XY. (2019) Resistance of gusset-tube DK-joints stiffened by 1/2 annular plates in transmission towers [J]. *Journal of Constructional Steel Research*, 159(C).
- [8]. Li F, Deng HZ, Hu XY. (2019) Design resistance of longitudinal gusset-tube K-joints with 1/4 annular plates in transmission towers [J]. *Thin-Walled Structures*, 144.
- [9]. Ju YZ, Li JY, Wang DH, Bai JF. (2018) Study of the Ultimate Load Capacity of K-Type Tube-Gusset Plate Connections [J]. *International Journal of Steel Structures*, 18(2).

- [10]. Qu SZ, Wu XH, Sun Q. (2018) Experimental and numerical study on ultimate behaviour of high-strength steel tubular K- joints with external annular steel plates on chord circumference [J]. Engineering Structures, 165.
- [11]. Yang ZY, Deng HZ. (2019) Analysis of Flexural Behavior of Steel Tube Tower Ring Ribbed Space Joint [J]. Journal of Tongji University (Natural Science Edition), 47(01):9-17.
- [12]. Yang ZY, Deng HZ, Hu XY. (2018) Strength of longitudinal X-type plate-to-circular hollow section (CHS) connections reinforced by external ring stiffener [J]. Thin-Walled Structures, 131.
- [13]. Yang ZY. (2015) Study on the force performance and ultimate bearing capacity of the node connecting the cross-stretcher and tower of steel pipe tower [D]. Shijiazhuang University of Railways.
- [14]. Zhang LJ, Li SC, He XW, Liu ZW, Wang ZY. (2021) Study on the influence of annular stiffening ribs on the bearing capacity and failure mode of large diameter coherent steel pipe nodes [J]. Industrial Building, 51(03):104-109.
- [15]. Kim WB, Shin KJ, Lee HD, Lee SH. (2015) Strength equations of longitudinal plate-to-circular hollow section (CHS) joints [J]. International Journal of Steel Structures, 15(2).
- [16]. Wang MH. (2014) Experimental research and theoretical study on bending capacity of tube-gusset K-joint connection [J]. Journal of Civil Engineering and Construction Technology, 5(2).

Acknowledgment

This work was supported by Henan Provincial Department of Science and Technology Research Project (222102320114) and Henan Provincial Department of Education Research Project (21B130002).